

FAST RADIO BURST DISCOVERED IN THE ARECIBO PULSAR ALFA SURVEY

L. G. SPITLER¹, J. M. CORDES², J. W. T. HESSELS^{3,4}, D. R. LORIMER⁵, M. A. MCLAUGHLIN⁵, S. CHATTERJEE², F. CRAWFORD⁶,
J. S. DENEVA⁷, V. M. KASPI⁸, R. S. WHARTON², B. ALLEN^{9,10,11}, S. BOGDANOV¹², A. BRAZIER², F. CAMILO^{12,13},
P. C. C. FREIRE¹, F. A. JENET¹⁴, C. KARAKO-ARGAMAN⁸, B. KNISPEN^{10,11}, P. LAZARUS¹, K. J. LEE^{1,15},
J. VAN LEEUWEN^{3,4}, R. LYNCH⁸, S. M. RANSOM¹⁶, P. SCHOLZ⁸, X. SIEMENS⁹, I. H. STAIRS¹⁷, K. STOVALL¹⁸,
J. K. SWIGGUM⁵, A. VENKATARAMAN¹³, W. W. ZHU¹⁷, C. AULBERT¹¹, AND H. FEHRMANN¹¹

¹ Max-Planck-Institut für Radioastronomie, D-53121 Bonn, Germany; lspliter@mpifr-bonn.mpg.de

² Department of Astronomy and Space Sciences, Cornell University, Ithaca, NY 14853, USA

³ ASTRON, Netherlands Institute for Radio Astronomy, Postbus 2, 7990 AA, Dwingeloo, The Netherlands

⁴ Anton Pannekoek Institute for Astronomy, University of Amsterdam, Science Park 904, 1098 XH, Amsterdam, The Netherlands

⁵ Department of Physics and Astronomy, West Virginia University, Morgantown, WV 26506, USA

⁶ Department of Physics and Astronomy, Franklin and Marshall College, Lancaster, PA 17604-3003, USA

⁷ Naval Research Laboratory, 4555 Overlook Ave SW, Washington, DC 20375, USA

⁸ Department of Physics, McGill University, Montreal, QC H3A 2T8, Canada

⁹ Physics Department, University of Wisconsin–Milwaukee, Milwaukee, WI 53211, USA

¹⁰ Leibniz Universität, Hannover, D-30167 Hannover, Germany

¹¹ Max-Planck-Institut für Gravitationsphysik, D-30167 Hannover, Germany

¹² Columbia Astrophysics Laboratory, Columbia University, New York, NY 10027, USA

¹³ Arecibo Observatory, HC3 Box 53995, Arecibo, PR 00612, USA

¹⁴ Center for Gravitational Wave Astronomy, University of Texas at Brownsville, Brownsville, TX 78520, USA

¹⁵ Kavli Institute for Astronomy and Astrophysics, Peking University, Beijing 100871, China

¹⁶ NRAO, Charlottesville, VA 22903, USA

¹⁷ Department of Physics and Astronomy, University of British Columbia, 6224 Agricultural Road, Vancouver, BC V6T 1Z1, Canada

¹⁸ Department of Physics and Astronomy, University of New Mexico, Albuquerque, NM 87131, USA

Received 2013 December 23; accepted 2014 May 19; published 2014 July 10

ABSTRACT

Recent work has exploited pulsar survey data to identify temporally isolated, millisecond-duration radio bursts with large dispersion measures (DMs). These bursts have been interpreted as arising from a population of extragalactic sources, in which case they would provide unprecedented opportunities for probing the intergalactic medium; they may also be linked to new source classes. Until now, however, all so-called fast radio bursts (FRBs) have been detected with the Parkes radio telescope and its 13-beam receiver, casting some concern about the astrophysical nature of these signals. Here we present FRB 121102, the first FRB discovery from a geographic location other than Parkes. FRB 121102 was found in the Galactic anti-center region in the 1.4 GHz Pulsar Arecibo *L*-band Feed Array (ALFA) survey with the Arecibo Observatory with a $DM = 557.4 \pm 2.0 \text{ pc cm}^{-3}$, pulse width of $3.0 \pm 0.5 \text{ ms}$, and no evidence of interstellar scattering. The observed delay of the signal arrival time with frequency agrees precisely with the expectation of dispersion through an ionized medium. Despite its low Galactic latitude ($b = -0^\circ.2$), the burst has three times the maximum Galactic DM expected along this particular line of sight, suggesting an extragalactic origin. A peculiar aspect of the signal is an inverted spectrum; we interpret this as a consequence of being detected in a sidelobe of the ALFA receiver. FRB 121102's brightness, duration, and the inferred event rate are all consistent with the properties of the previously detected Parkes bursts.

Key word: pulsars: general

Online-only material: color figures

1. INTRODUCTION

Radio pulsar surveys sample the sky at high time resolution and are thus sensitive to a range of time variability and source classes. Over the last decade, there has been renewed interest in expanding the purview of pulsar search pipelines, which traditionally exploit the periodic nature of pulsars, to also search for single dispersed pulses. This led to the discovery of rotating radio transients (RRATs; McLaughlin et al. 2006), which are believed to be pulsars that are either highly intermittent in their radio emission or have broad pulse-energy distributions that make them more easy to discover using this technique (Weltevrede et al. 2006). Of the now nearly 100 known RRATs,¹⁹ the vast majority emit multiple detectable pulses per hour of on-sky time, though a few have thus far produced only one observed pulse

(Burke-Spolaor & Bailes 2010; Burke-Spolaor et al. 2011b). The dispersion measures (DMs) of the RRATs are all consistent with a Galactic origin, according to the NE2001 model for Galactic electron density (Cordes & Lazio 2002).

Single-pulse search methods have also discovered a new class of fast radio bursts (FRBs) in wide-field pulsar surveys using the 13-beam, 1.4 GHz receiver at the Parkes radio telescope (Lorimer et al. 2007; Keane et al. 2012; Thornton et al. 2013). Most have been found far from the Galactic plane and have DMs that are anomalously high for those lines of sight. Lorimer et al. (2007) reported the first such burst with a Galactic latitude of $b = -42^\circ$ and $DM = 375 \text{ pc cm}^{-3}$. The expected DM contribution for that line of sight from the ionized interstellar medium (ISM) in our Galaxy is only 25 pc cm^{-3} according to the NE2001 model. The DM excess has been interpreted as coming from the ionized intergalactic medium (IGM) and led to the conclusion that FRBs are extragalactic.

¹⁹ <http://astro.phys.wvu.edu/rratalog/>

More recently, Thornton et al. (2013) reported four FRBs with Galactic latitudes of $|b| > 40^\circ$ and DMs ranging from 521 to 1072 pc cm⁻³. The expected Galactic DM contribution along the lines of sight of these bursts is 30–46 pc cm⁻³, i.e., only 3%–6% of the observed DM can be attributed to our Galaxy. An additional FRB candidate was reported by Keane et al. (2012) and is at a lower Galactic latitude ($b = -4^\circ$) than the other five reported Parkes FRBs. This source could be of Galactic origin given that the measured DM = 746 pc cm⁻³ is only 1.3 times the maximum expected DM from NE2001 along this line of sight. The dispersion delay of all of the published FRBs are consistent with the expected ν^{-2} dispersion law. Additionally, the burst reported by Lorimer et al. (2007) showed frequency-dependent pulse broadening that scaled as $\nu^{-4.8 \pm 0.4}$, consistent with the expected value of -4.0 to -4.4 (Lambert & Rickett 1999) for scattering by the ISM. The brightest burst reported by Thornton et al. (2013) showed a clear exponential tail and a pulse duration that scaled as $\nu^{-4.0 \pm 0.4}$. This provides additional credence to the interpretation that the signal is of astrophysical origin.

Generally, FRBs have been found in minute- to hour-long individual observations; multi-hour follow-up observations at the same sky positions have thus far failed to find repeated bursts. Thus, FRBs are considered a different observational phenomenon from RRATs based on DMs in excess of the predicted Galactic contribution and the fact that none of the FRBs has been seen to repeat. At this point, however, we cannot be certain that the bursts are non-repeating. Detecting an astrophysical counterpart will be an important step in determining whether we expect repeated events.

The progenitors and physical nature of the FRBs are currently unknown. The FRBs have brightness temperatures well in excess of thermal emission ($T_b > 10^{33}$ K) and therefore require a coherent emission process. One possible source of repeating, extragalactic FRBs is extremely bright, rare Crab-like giant pulses from extragalactic pulsars, which repeat over much longer time scales than currently constrained. Similarly Popov & Postnov (2007) propose hyperflares from extragalactic magnetars. Proposed extragalactic sources of non-repeating, fast radio transients include evaporating primordial black holes (Rees 1977), merging binary white dwarf systems (Kashiyama et al. 2013), merging neutron stars (Hansen & Lyutikov 2001), collapsing supramassive neutron stars (Falcke & Rezzolla 2014), and superconducting cosmic strings (Cai et al. 2012). Alternatively, Loeb et al. (2014) suggest a repeating, Galactic source—flares from nearby, magnetically active stars, in which the DM excess is due to the star’s corona. In this scenario, additional pulses could also be observed and potentially at a different DM. Localizing FRBs with arcsecond accuracy is technically challenging but will help identify potential host galaxies, or stars, and multi-wavelength counterparts.

In any pulsar survey, the vast majority of statistically significant signals are due to man-made radio frequency interference (RFI), which can originate far from the telescope or be locally generated. RFI can also mimic some of the characteristics of short-duration astronomical signals. Thus, care is needed when interpreting whether a particular signal is astronomical in origin, and claims of a new source class require due consideration and skepticism. The situation is further complicated by the discovery of “peryttons” (Burke-Spolaor et al. 2011a). Peryttons are short duration radio bursts observed in pulsar surveys over a narrow range of DMs but have patchy spectra and are observed in many beams simultaneously. The fact that FRBs have so far been observed with only the Parkes telescope has raised some

concern—even though the observed brightness distribution and event rate can explain why other experiments have so far not detected any similar signals.

In this article, we report the discovery of an FRB with the Arecibo Observatory. The FRB was found as part of the Pulsar ALFA (PALFA) survey of the Galactic plane (Cordes et al. 2006). This detection, made with a different telescope at a different geographic location, bolsters the astrophysical interpretation of a phenomenon seen until now only with Parkes. The outline for the rest of this paper is as follows. In Section 2, we describe the PALFA survey and the observations that led to the discovery of the new FRB. The burst’s properties are discussed in Section 3, and the implied FRB event rate is described in Section 4. A discussion of the possible origin of this FRB, both astrophysical and otherwise, is outlined in Section 5. In Section 6, we discuss the implications of our discovery for FRBs in general and present our conclusions.

2. OBSERVATIONS AND ANALYSIS

PALFA is a pulsar survey of the Galactic plane that uses the 305 m Arecibo telescope and the Arecibo *L*-band Feed Array²⁰ (ALFA; Cordes et al. 2006). ALFA is a seven-beam feed array with a single center pixel (beam 0) surrounded by a hexagonal ring of 6 pixels (beams 1–6) that spans the frequency range 1225–1525 MHz. The FWHM of each beam is approximately 3′5, and the beams are separated from each other by roughly one beam-width on the sky. (See Figure 1 for a map of the power pattern.) A tessellation of three pointings is required to sample the sky to the half-power point. The system temperature (T_{sys}) is 30 K. The on-axis gain of beam 0 is 10.4 K Jy⁻¹, and the average on-axis gain of the other six beams is 8.2 K Jy⁻¹. The peak gain of the sidelobes (about $\sim 5'$ from the beam centers) is 1.7 K Jy⁻¹, over twice as high as the on-axis gain of the Parkes beams. The 7 pixels yield an instantaneous field of view (FOV) of 0.022 deg² within the FWHM, though the effective FOV is larger as the sidelobes have enough sensitivity to detect FRBs.

The survey began in 2004 and targets low Galactic latitudes ($|b| \leq 5^\circ$) in two ranges of Galactic longitude: inner Galaxy ($30^\circ < l < 78^\circ$) and outer Galaxy ($162^\circ < l < 214^\circ$). Initially the PALFA survey data were recorded with the Wideband Arecibo Pulsar Processors (Dowd et al. 2000), and the single-pulse analysis of these data is presented in Deneva et al. (2009). In March of 2009, PALFA began observing with the Mock/PDEV²¹ spectrometers (hereafter Mock spectrometers). The Mock spectrometers cover the entire ALFA frequency range in two frequency subbands, which are separately recorded as 16-bit data. The 16-bit subband data are converted to 4-bit data to reduce storage requirements. The subbands are merged prior to processing and the resulting data have 322.6 MHz of bandwidth, 960 frequency channels, and a time resolution of 65.5 μ s. For a more detailed description of the Mock data, see, e.g., Lazarus (2013).

The time-frequency data are processed with a PRESTO²²-based pipeline to search for single dispersed pulses. The raw data are cleaned of RFI using the standard PRESTO RFI excision code (`rfifind`). The raw time-frequency data are dedispersed with 5016 trial DMs ranging from DM = 0–2038 pc cm⁻³;

²⁰ <http://www.naic.edu/alfa/>

²¹ <http://www.naic.edu/~phil/hardware/pdev/usersGuide.pdf>

²² <http://www.cv.nrao.edu/~sransom/presto/>

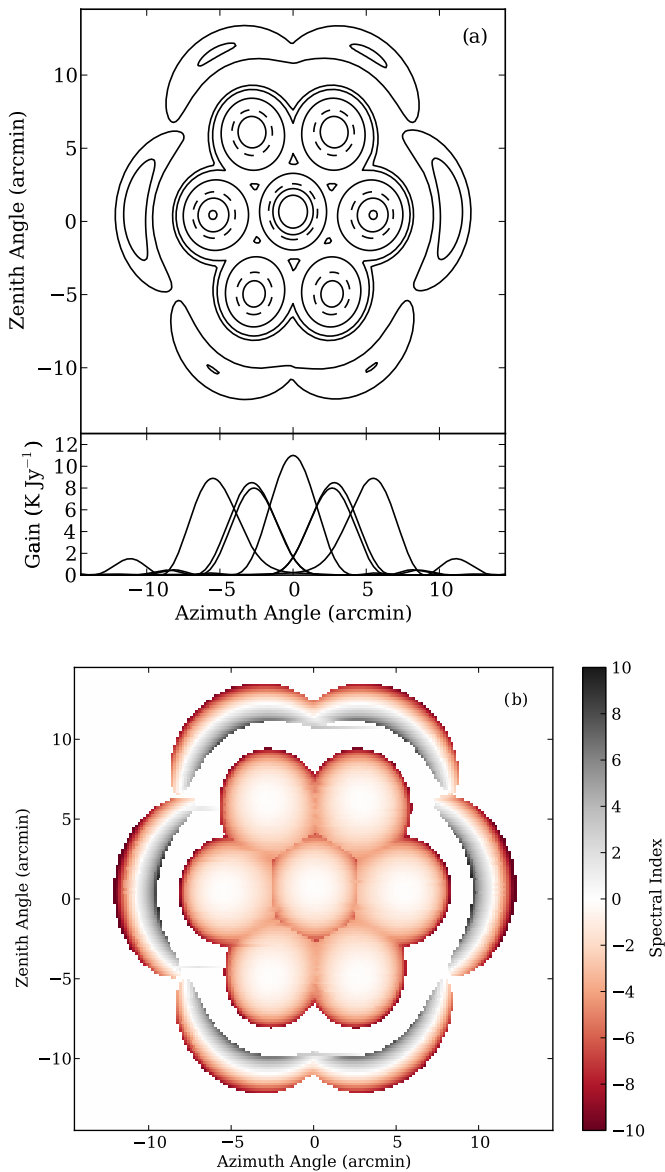


Figure 1. Gain and spectral index maps for the ALFA receiver. (a) Contour plot of the ALFA power pattern at $\nu = 1375$ MHz, calculated from the model described in Section 3. The contour levels are -13 , -10 , -6 , -3 (dashed), -2 , and -1 dB (top panel). The bottom inset shows slices in azimuth for each beam, and each slice passes through the peak gain for its respective beam. Beam 1 is in the upper right, and the beam numbering proceeds clockwise. Beam 4 is, therefore, in the lower left. (b) Map of the apparent instrumental spectral index due to frequency-dependent gain variations of ALFA. The spectral indexes were calculated using the center frequencies of each subband. Only pixels with gain > 0.5 K Jy^{-1} were used in the calculation. The rising edge of the first sidelobe can impart a positive apparent spectral index with a magnitude that is consistent with the measured spectral index of FRB 121102. Note that the orientation of the beams in this figure does not reflect the actual orientation during the observations. The feed was rotated by 19° with respect to north-south, and the zenith angle at the time of the observation was 16.5° .

(A color version of this figure is available in the online journal.)

the maximum DM searched is roughly twice as high as the maximum Galactic DM contribution expected for any line of sight covered in the survey. Single pulse candidates are identified in each dedispersed time series using a matched filtering algorithm (`single_pulse_search.py`). This algorithm increases the sensitivity to pulses wider than the original time resolution of the data by convolving each dedispersed time series with a series of boxcar matched filters (for a general discussion of this

Table 1
Observational Parameters of FRB 121102

Parameter	Value
Date	2012 Nov 2
Time	06:35:53 UT
MJD arrival time ^a	56233.27492180
Right ascension ^b	05 ^h 32 ^m 09 ^s .6
Declination ^b	33°05′13″.4
Gal. long.	174°95
Gal. lat.	$-0^\circ 223$
DM (pc cm^{-3})	557.4 ± 2.0
DM _{NE2001,max} (pc cm^{-3})	188
Dispersion index, ^c β	-2.01 ± 0.05
Pulse width (ms)	3.0 ± 0.5
Pulse broadening (ms), ^d τ_d	< 1.5
Flux density (Jy), ^e S	$0.4^{+0.4}_{-0.1}$
Spectral index range, ^f α	7 to 11

Notes.

^a Barycentered arrival time referenced to infinite frequency.

^b The J2000 position of the center of beam 4.

^c Dispersive time delay $\propto \nu^\beta$.

^d At 1 GHz.

^e Flux estimation at 1.4 GHz assumes a sidelobe detection and a corresponding gain of 0.7 ± 0.3 K Jy^{-1} .

^f $S(\nu) \propto \nu^\alpha$.

technique, see Cordes & McLaughlin 2003). After matched filtering, pulse candidates are identified by applying a threshold signal-to-noise ratio ($S/N > 5$). The spectral modulation index statistic was calculated for each event to identify those caused by narrowband RFI (Spitler et al. 2012). Candidate pulses are identified by inspecting a standard set of single-pulse diagnostic plots (e.g., Figures 5 and 6 in Cordes & McLaughlin 2003). In practice, an isolated pulse needs an S/N somewhat above the threshold ($S/N \gtrsim 7$) in order to verify that it is astrophysical. A repeated source of pulses found at an S/N close to the threshold, for example, from an RRAT, could be recognized as astrophysical because of the underlying periodicity.

The analysis presented here includes data recorded with the Mock spectrometers from beginning with their deployment in 2009 March through 2012 December, for a total of ~ 5045 pointings in the outer Galaxy. The distribution in Galactic latitude of the pointings is fairly uniform so far; the number of pointings in 1° bins from $|b| = 0^\circ - 5^\circ$ is 8134, 5926, 7252, 7476, and 6279, respectively. For this analysis we do not consider the inner Galaxy pointings because the larger DM contribution makes finding extragalactic bursts more difficult. The outer Galaxy observations are conducted in piggy-back mode with our commensal partners, and pointing duration varies depending on their requirements. Roughly 70% of the pointings have a duration of 176 s, and 30% have a duration of 268 s. The total observing time of all the pointings is 283 hr, or 11.8 days.

3. FRB 121102 BURST DESCRIPTION

A single, dispersed pulse with an $S/N = 14$ was observed in ALFA beam 4 on 2012 November 2 (MJD = 56233.27492180) at 06:35:53 UT in a 176 s survey pointing toward the Galactic anticenter. Because we do not know for certain where in the beam the burst occurred, we give the position to be the center of beam 4 ($b = -0^\circ 223, l = 174^\circ 95$). The burst occurred 128 s into the observation. The burst properties are summarized in Table 1. Following the naming convention introduced by Thornton et al.

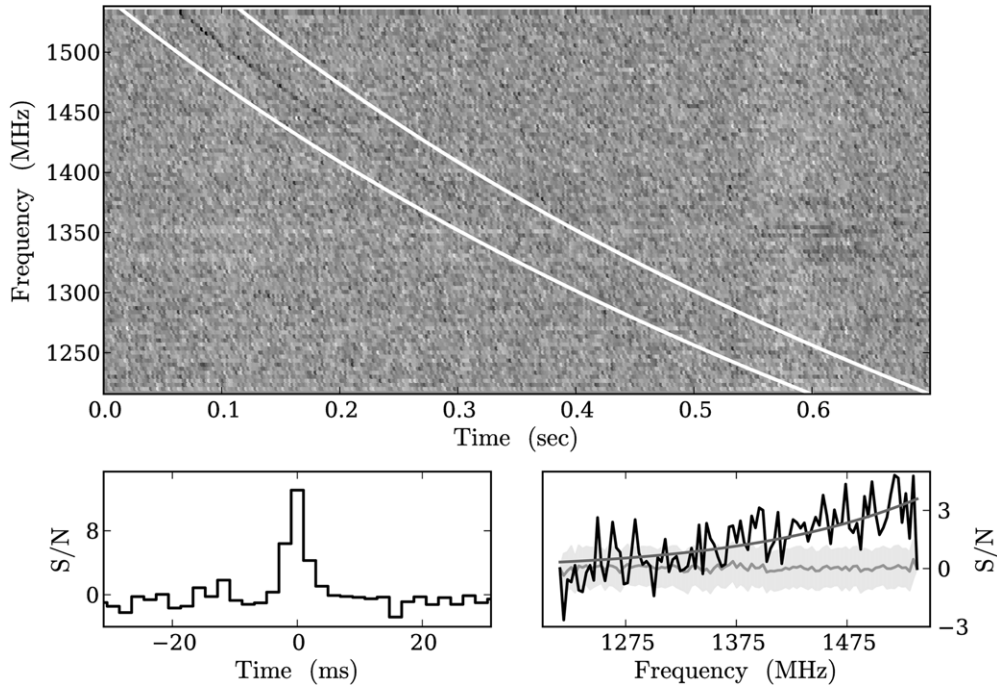


Figure 2. Characteristic plots of FRB 121102. In each panel, the data were smoothed in time and frequency by a factor of 30 and 10, respectively. The top panel is a dynamic spectrum of the discovery observation showing the 0.7 s during which FRB 121102 swept across the frequency band. The signal is seen to become significantly dimmer toward the lower part of the band, and some artifacts due to RFI are also visible. The two white curves show the expected sweep for a ν^{-2} dispersed signal at a $DM = 557.4 \text{ pc cm}^{-3}$. The lower left panel shows the dedispersed pulse profile averaged across the bandpass. The lower right panel shows the on-pulse spectrum (black), and for reference, a curve showing the fitted spectral index ($\alpha = 10$) is also overplotted (medium gray). The on-pulse spectrum was calculated by extracting the frequency channels in the dedispersed data corresponding to the peak in the pulse profile. For comparison, the median value (gray line) and standard deviation (light gray region) of each frequency channel was calculated in an off-pulse region roughly 0.5 s before and after the pulse.

(2013), we henceforth refer to this event as FRB 121102. A frequency versus time plot of the pulse, a dedispersed pulse profile, and the spectrum of the pulse are shown in Figure 2.

The DM of the pulse was calculated using a standard analysis technique also employed in pulsar timing. The data were divided into 10 frequency subbands and times of arrival were determined from the five highest frequency subbands. The lower five subbands were not included because the S/N was too low. The best-fit DM is $557.4 \pm 2.0 \text{ pc cm}^{-3}$. The NE2001 model predicts a maximum line of sight Galactic DM of 188 pc cm^{-3} , i.e., roughly one-third of the total observed column density. For comparison, PSR J0540+3207 has the larger DM of the two known pulsars within 5° of FRB 121102 with a DM of 62 pc cm^{-3} (Manchester et al. 2005) and a DM-derived distance of 2.4 kpc.

We also explored the possibility of a sweep in frequency that deviates from the standard ν^{-2} expected from dispersion in the ionized ISM, i.e., ν^β , where β is the DM index. The DM-fitting analysis described above determined a best fit for the DM index of $\beta = -2.01 \pm 0.03$. Also, a least-squares fit for deviations from the ν^{-2} law verified that a variation in β from -2 of up to 0.05 can be tolerated given the time resolution of the data. We also note that the value of DM is for $\beta = 2$ because the units are otherwise inappropriate. As such, we report a final value of DM index of $\beta = -2.01 \pm 0.05$.

The remaining burst properties were determined by a least-squares fit of the time-frequency data with a two-dimensional pulse model doing a grid search over a range of parameters. The model assumes a Gaussian pulse profile convolved with a one-sided exponential scattering tail that is parameterized by a $1/e$ temporal width τ_d . The amplitude of the Gaussian is scaled with

a spectral index ($S(\nu) \propto \nu^\alpha$), and the temporal location of the pulse was modeled as an absolute arrival time plus dispersive delay. For the least-squares fitting the DM was held constant, and the spectral index of τ_d was fixed to be -4.4 . The Gaussian FWHM pulse width, the spectral index, Gaussian amplitude, absolute arrival time, and pulsar broadening were all fitted. The Gaussian pulse width (FWHM) is $3.0 \pm 0.5 \text{ ms}$, and we found an upper limit of $\tau_d < 1.5 \text{ ms}$ at 1 GHz. The residual DM smearing within a frequency channel is 0.5 ms and 0.9 ms at the top and bottom of the band, respectively. The best-fit value of the spectral index was $\alpha = 11$ but could be as low as $\alpha = 7$. We note that the fit for α is highly covariant with the Gaussian amplitude.

Every PALFA observation yields many single-pulse events that are not associated with astrophysical signals. A well-understood source of events is false positives from Gaussian noise. These events are generally isolated (i.e., no corresponding event in neighboring trial DMs), have low S/Ns, and narrow temporal widths. RFI can also generate a large number of events, some of which mimic the properties of astrophysical signals. Nonetheless, these can be distinguished from astrophysical pulses in a number of ways. For example, RFI may peak in S/N at $DM = 0 \text{ pc cm}^{-3}$, whereas astrophysical pulses peak at a $DM > 0 \text{ pc cm}^{-3}$. Although both impulsive RFI and an astrophysical pulse may span a wide range of trial DMs, the RFI will likely show no clear correlation of S/N with trial DM, while the astrophysical pulse will have a fairly symmetric reduction in S/N for trial DMs just below and above the peak value. RFI may be seen simultaneously in multiple, non-adjacent beams, while a bright, astrophysical signal may only be seen in one beam or multiple, adjacent beams. FRB 121102 exhibited all of

the characteristics expected for a broadband, dispersed pulse, and therefore clearly stood out from all other candidate events that appeared in the pipeline output for large DMs.

We also performed a thorough periodicity search on the discovery observation. We created a set of trial dedispersed time series around the burst DM, using an `rfifind` mask to excise RFI. Each trial DM was searched for periodicities using PRESTO's `accelsearch` and all candidate signals with an S/N greater than 3σ were folded and inspected by eye. This closer inspection, in addition to the blind periodicity search that had already been done as part of the normal survey processing, also failed to reveal any periodic candidates.

Reobservations of the source position showed no additional pulses at the discovery DM. First, the same seven-beam ALFA survey pointing direction was repeated in a 176 s observation on 2012 November 4. Second, targeted follow-up was done using the L-wide single-pixel receiver and the PUPPI spectrometer on 2013 July 7, during which the position of beam 4 was observed continuously for 1.66 hr. The L-wide receiver has a frequency range of 1.15–1.73 GHz and an FWHM of $3/5$, while PUPPI provides a time resolution of 40.96 μ s and a bandwidth of 800 MHz, which was divided into 2048 frequency channels. These data were processed using the single-pulse search algorithms and a narrow range of DMs spanning the burst's DM.

Finally, because the uncertainty on the position of FRB 121102 is larger than the FWHM of the ALFA beams, we performed a dense sampling of the region around the original beam 4 pointing center using three interleaved ALFA pointings of 2600 s each and recorded with the Mock spectrometers on 2013 December 9–10. Combined, these covered a circular area with an approximate diameter of $17'$. An additional 2385 s observation was conducted on 2013 December 10 using the Arecibo 327 MHz receiver and the PUPPI backend with the telescope pointed at the center of the beam 4 position from the discovery observation. The FWHM of the beam of the 327 MHz receiver is $14'$, so this observation covered both the position of the main beam and sidelobe of ALFA. The lower frequency observation was performed in the event that the single bright burst seen at 1.4 GHz was part of a broad distribution of pulses emitted from a source with a steep negative spectral index, as expected for pulsar-like coherent radiation. These observations were searched for single pulses over a narrow DM range and also for periodic signals at the burst's DM. No additional bursts or periodic astrophysical signals were found.

One peculiar property of FRB 121102 is the observed positive apparent spectral index of $\alpha = 7$ –11. If the coherent emission process for FRBs is similar to that of pulsars, we would expect an intrinsically negative spectral index or a flat spectral index in the case of magnetars. The spectral indices of the Thornton et al. (2013) bursts are consistent with being flat. We therefore suspect that the observed positive spectral index is caused by frequency-dependent gain variations of ALFA. To explore this possibility, we developed a model for the receiver using an asymmetric Airy function and coma lobes but no correction for blockage from the feed support structure. The left panel of Figure 1 is a map of ALFA's power pattern using this model. We also generated a map of the induced spectral index at the center frequencies of the two Mock subbands. The spectral index map is shown in the right panel of Figure 1. Most positions within the beam pattern, including the entire main beam, impart a negative spectral index. However, the rising edge of the first sidelobe can impart a positive spectral index bias of $0 \lesssim \alpha \lesssim 10$.

We therefore conclude that the burst was likely detected in the sidelobe and not the main beam. Note that we see no evidence for the burst in the co-added dedispersed time series from pairs of neighboring beams (beams 0 and 3 and beams 0 and 5) with $S/N > 4$.

It is also possible that the observed spectrum is additionally biased by RFI. Indeed, the lower of the two Mock subbands is significantly more affected by RFI contamination compared with the upper subband, which may contribute partly to the observed positive spectral index. In summary, given the uncertainty in the exact position, as well as the exact beam shape and other extrinsic effects, it is unfortunately impossible to adequately constrain the true spectral index of the burst.

Nonetheless, the sidelobe detection hypothesis allows us to better constrain both the position and flux of the burst. Conservatively, we consider a range of gain corresponding to the inner edge of the sidelobe of 0.4 – 1.0 K Jy $^{-1}$ for a mean gain of 0.7 K Jy $^{-1}$. Estimating the peak flux density (S) from the radiometer equation, we have $S = 0.4_{-0.1}^{+0.4}$ Jy, where we have assumed $S/N = 14$, $T_{\text{sys}} = 30$ K, a bandwidth of 300 MHz, and a pulse duration of 3 ms. If instead FRB 121102 was detected on axis, the flux density is ~ 40 mJy, which is an order of magnitude weaker than any other known FRB.

4. EVENT RATE ANALYSIS

We can estimate the occurrence rate of FRBs from our single FRB discovery, the total observing time included in this analysis, and the instantaneous FOV of ALFA. The gain variations of the receiver (see Figure 1) complicate the definition of the instantaneous FOV, but a practical definition is the region enclosed by a minimum system gain threshold. We calculate the rate using two different assumptions for minimum gain. The first is the area enclosed by the FWHM level of the seven beams (Ω_{FWHM}), and because the sidelobes of Arecibo have comparable sensitivity to Parkes, we also assume a lower minimum gain that encompasses the main beams and first sidelobes ($\Omega_{\text{MB+SL}}$). We use the numerical model of the ALFA beam pattern shown in Figure 1 to calculate the instantaneous FOV and a FOV-averaged system equivalent flux density S_{sys} .

The FWHM FOV is defined to be the area with a gain greater than half the peak gain of the outer beams, i.e., where $G > 4.1$ K Jy $^{-1}$. This corresponds to $\Omega_{\text{FWHM}} = 0.022$ deg 2 and an FOV-averaged $S_{\text{sys}} = 5$ Jy. Using the radiometer equation, a fiducial pulse width of 1 ms, a bandwidth of 300 MHz, two summed polarizations, and $S/N = 10$, we get that $S_{\text{min}} = 65$ mJy. For 11.8 days of observing, the event rate is then $R_{S>65 \text{ mJy}} = 1.6_{-1.5}^{+6} \times 10^5$ sky $^{-1}$ day $^{-1}$. The uncertainty interval represents the 95% confidence interval assuming the occurrence of FRBs is Poisson distributed.

The main beam and sidelobe FOV was defined as the region with $G > 0.4$ K Jy $^{-1}$. This value of gain was chosen because it corresponds to the average FWHM sensitivity of the Parkes multibeam receiver. The instantaneous FOV is $\Omega_{\text{MB+SL}} = 0.109$ deg 2 , and the FOV-averaged $S_{\text{sys}} = 27$ Jy. Using the same parameters as above yields a minimum detectable flux density of $S_{\text{min}} = 350$ mJy. The corresponding event rate is then $R_{S>350 \text{ mJy}} = 3.1_{-3.1}^{+12} \times 10^4$ sky $^{-1}$ day $^{-1}$.

Thornton et al. (2013) have the most robust event rate of FRBs published to date with $R_{S3 \text{ Jy}} = 1_{-0.5}^{+0.6} \times 10^4$ day $^{-1}$ sky $^{-1}$ for a 1 ms burst. To determine whether this rate is consistent with our inferred rates, one must consider the relative volumes probed given each survey's S_{min} . If the FRBs do come from

a population of sources at $z \gtrsim 1$, one must also account for cosmological effects, i.e., simple Euclidean geometry is no longer valid. Lorimer et al. (2013) introduce a model for the FRB population that properly handles the effect of cosmology on the detection rate, and for concreteness, they scale their predictions to the Thornton et al. (2013) FRB properties. Scaling our event rates using this prescription, we find that our inferred rates are roughly consistent with the cosmological model, but we caution that the model is predicated on a large number of uncertain assumptions. In particular, the distance (or redshift) of a burst is estimated from the observed DM and requires making an assumption about the contribution of the host Galaxy, which is highly uncertain. Furthermore, the intrinsic emission properties of the FRBs (e.g., spectral index, beaming fraction) is also known.

5. ORIGIN OF THE PULSE

In this section, we describe three possible origins for FRB 121102: terrestrial, Galactic, or extragalactic. To avoid confusion, we adopt different nomenclature for the two astrophysical possibilities, namely, FRBg and FRBx for FRBs originating from Galactic and extragalactic sources, respectively.

5.1. Terrestrial

One possible terrestrial cause of FRB 121102 is RFI, but there are many reasons why this is unlikely. First, the burst was seen in only a single ALFA beam. Strong signals due to RFI are generally seen in several or all beams simultaneously due to their local origin (Burke-Spolaor et al. 2011a). To verify that this burst was localized to a single beam, we co-added the dedispersed time series for all beams except beam 4 and applied the same single-pulse detection algorithms described in Section 2. This resulted in no detected pulses contemporaneous with the beam 4 signal at an S/N > 4. Second, the frequency dependence of the dispersion sweep of FRB 121102 was measured to be -2.01 ± 0.05 , which is statistically consistent with the expected value of -2 for the propagation of a radio wave in the ISM. This simple relation is known to hold extremely well along Galactic lines of sight (Hassall et al. 2012). Last, since there are no similar, isolated high-DM signals detected in our data set, an RFI interpretation would also require this to be quite an unusual event.

Another possible terrestrial source are the so-called ‘‘peryttons.’’ Peryttons are broadband radio bursts discovered with the Parkes multibeam receiver (Burke-Spolaor et al. 2011a; Kocz et al. 2012; Bagchi et al. 2012). They have typical durations of ~ 30 – 50 ms (10 times longer than FRBs) and have patchy spectra. They are dispersed in frequency with a narrow range of timescales (equivalent DMs of ~ 375 pc cm $^{-3}$) but with dispersive frequency scalings that are not always consistent with ν^{-2} . Most notably, they are seen in many beams simultaneously and are believed to be sidelobe detections of a bright source (Burke-Spolaor et al. 2011a) or near-field detections of atmospheric emission (Kulkarni et al. 2014). Also, if peryttons are caused by an atmospheric phenomenon in the near-field, Kulkarni et al. (2014) show that a detection in a single beam by Arecibo would exclude the possibility that peryttons and FRBs are the same phenomena. Whether the source is man-made or natural is still unclear.

The observed properties of FRB 121102 are inconsistent with those of peryttons. The flux density of FRB 121102 decreases

smoothly with decreasing frequency until it drops below the noise level, and is therefore different than the patchy perytton spectra in which the signal fades in and out across the bandpass. The temporal widths of the peryttons are at least ten-times larger than FRB 121102. The dispersive sweeps of the peryttons are at least two times shorter than our FRB (per unit frequency). Perhaps most importantly, our burst was only seen in a single ALFA beam, while the peryttons were always seen in multiple or all Parkes beams. We also note that we were explicitly looking for astrophysical-like signals, i.e., those that appear only in one or up to three neighboring beams. Our apparent non-detection of peryttons should not be taken as a strong statement on their existence, as we were not looking for them.

5.2. Galactic

Because the observed DM is only three times the predicted DM from the NE2001 model (188 pc cm $^{-3}$), it is conceivable that FRB 121102 is an FRBg, and the DM excess is caused by localized density enhancements along the line of sight. We have investigated the possibility of unmodeled gas by checking H α and H II survey catalogs. The position of FRB 121102 was mapped by the Wisconsin H α Mapper Northern Sky Survey (Haffner et al. 2003) with 1 $^\circ$ spatial resolution (see also Finkbeiner 2003). The emission measure (EM) inferred from the H α intensity is EM = 28 pc cm $^{-6}$ using the expression from Haffner et al. (1998; assuming $T = 10^4$ K, $I_{\text{H}\alpha} \approx 10$ R, and no extinction). For this line of sight, the NE2001 model predicts EM = 15–70 pc cm $^{-6}$ assuming an outer scale for the electron-density spectrum of 10–100 pc, which is appropriate for the thick disk in the outer Galaxy. The consistency between the measured EM and predicted EM suggests that NE2001 is correctly modeling the electron content for line of sight, and therefore the predicted DM is also accurate.

We also checked for H II regions along the line of sight by searching through two complementary catalogs. Paladini et al. (2003) compiled a catalog of 1442 H II regions from 24 previously published radio surveys, and Anderson et al. (2014) produced a catalog of over 8000 known and candidate H II regions using infrared images from the *Wide-Field Infrared Survey Explorer* and archival radio data. The closest H II region in either catalog was greater than 1 $^\circ$ away from the position of FRB 121102. In conclusion, we find no evidence for previously unmodeled dense gas along the line of sight that would explain the excess DM.

Figure 3 illustrates the Galactic DM excess for pulsars and FRBs quantified by the DM ratio, $r_{\text{DM}} = \text{DM}_{\text{obs}} / \text{DM}_{\text{NE2001,max}}$, where DM_{obs} is the observed DM for a source and $\text{DM}_{\text{NE2001,max}}$ is the DM expected for the source’s line of sight integrated through the entire Galaxy. Four classes of sources are included: Galactic pulsars, RRATs, pulsars in the Small and Large Magellanic Clouds (SMC and LMC), and FRBs. The data for the Galactic, SMC, and LMC pulsars are from the ATNF Pulsar Catalog²³ (Manchester et al. 2005). The RRAT data are from the RRATalog, and the FRB data are from this paper, Lorimer et al. (2007), Keane et al. (2012), and Thornton et al. (2013).

Galactic pulsars have $r_{\text{DM}} < 1$, except for a few pulsars whose observed DM is likely enhanced due to unmodeled local excesses in the ISM (e.g., H II regions). While this may suggest the DM excess of FRB 121102 could also be due to uncertainties in the NE2001 model, our analysis of H α and H II data described above makes this highly unlikely. The six

²³ <http://www.atnf.csiro.au/people/pulsar/psrcat/>

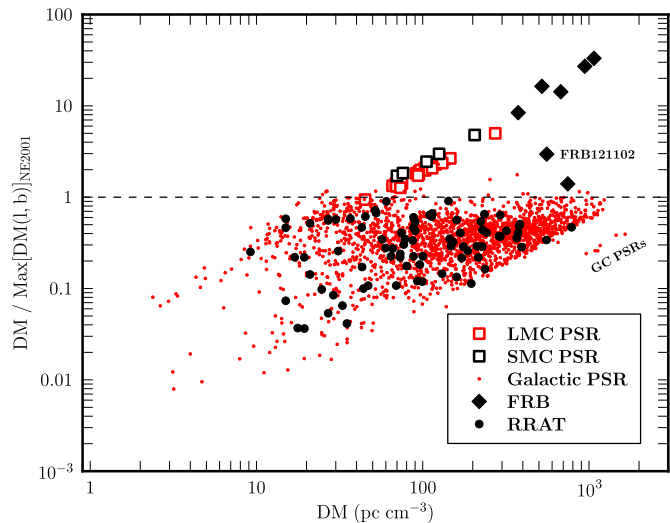


Figure 3. Ratio (r_{DM}) of measured DM to maximum Galactic dispersion measure plotted against measured DM. The maximum Galactic DM is calculated by integrating the NE2001 model to the edge of the Galaxy for each pulsar line of sight. The dashed line shows the maximum unity ratio expected for Galactic objects if the electron density is accurate for all lines of sight. The six pulsars near the GC are clustered on the far right of the plot. The RRATs have DM ratios consistent with the rest of the Galactic pulsar population. Known pulsars in the LMC and SMC have $r_{DM} \sim 1$ –5, and the seven FRBs have ratios from 1.2 to 33. The Keane et al. (2012) burst has the lowest DM ratio of the FRBs and is located to the lower right of FRB 121102. The Lorimer et al. (2007) burst and the Thornton et al. (2013) bursts fall along the line that extends from the LMC and SMC pulsars with the Lorimer et al. (2007) burst being the left-most point. (See Section 5 for data source references.)

(A color version of this figure is available in the online journal.)

known pulsars within ~ 100 pc of the Galactic center (GC) are clustered at $DM \sim 1000$ pc cm $^{-3}$ and $r_{DM} \sim 0.2$ –0.4 and are offset in DM from the rest of the pulsar population due to the increased density of the ionized ISM in the GC. RRATs have DM ratios consistent with Galactic pulsars. The pulsars in the LMC and SMC have $r_{DM} = 1$ to 5, reflecting the additional contribution of the ionized electrons in the LMC, SMC, and possibly from the local IGM. The FRB from Keane et al. (2012) has the lowest DM ratio, which is lower even than some of the Galactic pulsars, suggesting this burst could be Galactic. In fact Bannister & Madsen (2014) infer that this FRB is Galactic with a 90% probability from an EM determined using optical spectroscopy. The five, high-Galactic-latitude bursts from Lorimer et al. (2007) and Thornton et al. (2013) have DM ratios greater than even the Magellanic Clouds, which makes a Galactic interpretation difficult. The LMC and SMC pulsars and high-Galactic-latitude FRBs fall long a line because the maximum Galactic DM contribution at high Galactic latitudes is roughly constant ($DM \sim 50$ pc cm $^{-3}$). The DM ratio of FRB 121102 is larger than all of the Galactic pulsars, but only just. We also note that the inferred extragalactic DM contribution for FRB 121102 is ~ 370 pc cm $^{-3}$, which is larger than for the FRB from Lorimer et al. (2007).

If the burst is an FRBg, the most likely source is an RRAT. RRATs have been observed with only one pulse in an epoch (Burke-Spolaor & Bailes 2010; Burke-Spolaor et al. 2011b). However, our lack of a detection in the 327 MHz follow-up observations suggests that FRB 121102 is not simply an unusually bright pulse of an otherwise weak pulsar. While we cannot completely rule out that this burst is an FRBg, it is highly unusual for Galactic sources.

5.3. Extragalactic

The final possibility is that FRB 121102 is an extragalactic burst. The root of this interpretation is an observed DM in excess of the expected Galactic DM. With their large DM excesses, the four Thornton et al. (2013) bursts are the most convincing examples of FRBs, and most of the properties of FRB 121102 are similar to these bursts. Only the positive, observed spectral index is inconsistent with these FRBs, but as explained in Section 3, this can be an instrumental effect. FRB 121102’s observed pulse width is consistent with those of the known population of FRBs, which have observed durations of ~ 1 –8 ms, and like FRB 121102, they generally show little to no scattering (Thornton et al. 2013; Keane et al. 2012).

In Section 3, we derived a peak pulse flux density of $S = 0.4^{+0.4}_{-0.1}$ Jy for FRB 121102 (assuming it was detected in a sidelobe). The flux of FRB 121102 is therefore consistent with the peak flux densities of 0.4–1.3 Jy for bursts reported by Thornton et al. (2013) and 0.4 Jy reported by Keane et al. (2012). On the other hand, the original Lorimer et al. (2007) FRB 010724 had a peak flux density (~ 30 Jy) that is still more than an order-of-magnitude larger than those discovered since.

The PALFA survey has to date discovered only six pulsars in the outer Galaxy, and none of them are RRATs.²⁴ The outer Galaxy discovery with the highest DM is J0627+16 with $DM = 113$ pc cm $^{-3}$. FRB 121102 is therefore quite different than the other discoveries by PALFA in this region.

In summary, FRB 121102 shares many of the same observational properties with FRBs believed to be extragalactic, and the occurrence rate is consistent with previous discoveries. Therefore we believe that the Arecibo FRB is also likely extragalactic.

6. DISCUSSION AND CONCLUSIONS

Under the assumption that FRB 121102 is extragalactic in origin, and following Thornton et al. (2013), we can estimate the redshift, z , of the burst based on the observed total dispersion delay across the bandpass, which is fortuitously for ALFA ~ 1 ms for each 1 pc cm $^{-3}$ of DM, i.e., $\Delta t_{\text{obs}} = 552$ ms (Figure 2). The contributions to Δt_{obs} are from (1) free electrons in the Galactic ISM (Δt_{ISM}); (2) the IGM (Δt_{IGM}); (3) the putative host galaxy (Δt_{Host}). Adopting the NE2001 electron density for this line of sight, we find $\Delta t_{\text{ISM}} \simeq 184$ ms. To be consistent with the estimates presented in Thornton et al. (2013), we make the same assumptions about Δt_{IGM} and Δt_{Host} as presented in their Figure S3. Using the model DM scaling relationship for the IGM model of Ioka (2003) and Inoue (2004), we find $\Delta t_{\text{IGM}} \simeq 1200 z$ ms. For a host galaxy DM contribution of 100 pc cm $^{-3}$, $\Delta t_{\text{Host}} \simeq 100 \text{ ms}/(1+z)^2$. The condition $\Delta t_{\text{obs}} = \Delta t_{\text{ISM}} + \Delta t_{\text{IGM}} + \Delta t_{\text{Host}}$ is met when $z = 0.26$. The redshift value can be taken as an upper bound because it is plausible that a host galaxy can contribute more to the total delay than we have assumed. As was the case for the redshift estimates presented by Thornton et al. (2013; $z = 0.45$ –0.96), the contributions to Δt_{obs} are highly model dependent, and therefore the z value should be used with caution.

With these caveats in mind, the implied co-moving radial distance at $z = 0.26$ would be $D \sim 1$ Gpc. The FRB pseudo-luminosity $SD^2 \sim 1 \times 10^{12}$ Jy kpc 2 and energy output is $\sim 10^{38}$ erg for isotropic emission and $\sim 10^{37}$ erg for emission beamed over 1 sr. Both values are consistent with the FRBs from Thornton et al. (2013). Using this estimate of the co-moving

²⁴ <http://www.naic.edu/~palfa/newpulsars/>

distance, we can also constrain the brightness temperature, i.e., $T_b \sim 1 \times 10^{34} D_{\text{Gpc}}^2 \text{ K}$, where D_{Gpc} is the source distance in units of Gpc. This unphysically large brightness temperature requires a coherent emission process.

All of the FRBs observed to date show less temporal scattering than pulsars with similar DMs. Using a population of pulsars at low Galactic latitudes, Bhat et al. (2004) determined an empirical relation for pulse broadening timescale versus DM and observing frequency. For example, the predicted pulse broadening timescales for $\text{DM} = 500\text{--}1000 \text{ pc cm}^{-3}$ are 2–2000 ms at 1.4 GHz, albeit with a large scatter in the observed distribution. By comparison, only FRB 110220 has a measurable scattering timescale of $\sim 5 \text{ ms}$ with $\text{DM} = 910 \text{ pc cm}^{-3}$ (Thornton et al. 2013), roughly a factor of 200 less than predicted by Bhat et al. (2004). Using this single FRB scattering measurement, Lorimer et al. (2013) scale the Bhat et al. (2004) relation. The scaled relation predicts a scattering timescale for FRB 121102 of $\sim 0.04 \text{ ms}$, which is shorter than the time resolution of the data. If this relation can in fact be applied broadly to FRBs, then it is not surprising that we detected no scattering. Lorimer et al. (2013) point out that for a given scattering screen, the largest observed scattering occurs when the screen is near the mid-point between the source and observer, due to geometric effects. This suggests that the IGM or an intervening galaxy located midway along the line of sight would be the most important contribution to the scattering of FRBs. However, Cordes & McLaughlin (2003) show that for a source imbedded in a region of high scattering, for example near the center of the host galaxy or for a line of sight that passes through the host’s galactic disk, the observed scattering can still be dominated by the host galaxy even at large distances. Observations of scattering along extragalactic lines of sight by Lazio et al. (2008) and more theoretical calculations by Macquart & Koay (2013) suggest that scattering in the IGM is several orders of magnitude lower than in the ISM, which is consistent with the observations of FRBs.

One caveat to the conclusions of this paper is that the search presented here, and all searches for dispersed radio bursts, are optimized for signals with a ν^{-2} dispersive time delay. This simple approach introduces a selection effect in what signals breach the S/N threshold used to identify candidates, and thus which signals are deemed worthy of close inspection. We note, however, that this selection effect is not severe in our case as the fractional bandwidth we have used here (20%) is just barely sufficient to see the quadratic curvature of the burst delay.

Although the poor localization of FRB 121102 prevents a detailed search for a multi-wavelength counterpart, we searched for any major high-energy events that were both contemporaneous and co-located on the sky. We checked the Gamma-ray Coordinates Network archive of γ -ray bursts and found no potential association with FRB 121102. There are no plausible associations with X-ray transients detected by current all-sky monitors, and there are no observations of the field of FRB 121102 (within a $20'$ radius) with X-ray telescopes. There is no source associated with the position of FRB 121102 in either the *ROSAT* All Sky Survey Catalog or the *Fermi* Source Catalog.

In summary, we have described the Arecibo discovery of FRB 121102, a single, highly dispersed pulse in the PALFA survey. This is the first claimed FRB detection that has been found with a telescope other than Parkes. The large DM excess, roughly three times what would be expected from the Galactic ISM along this line of sight, the absence of repeat bursts, and the low measured interstellar scattering suggest that this is an FRBx and

not a Galactic emitter such as an RRAT. Using the event rate inferred from the PALFA discovery, there is the potential in the coming years to find two to three more FRBs in the remaining outer Galaxy survey region.

We thank the referee for extensive comments that significantly improved the clarity of this paper. We thank M. Kramer, B. Stappers, and R. Ekers for useful discussions. The Arecibo Observatory is operated by SRI International under a cooperative agreement with the National Science Foundation (AST-1100968), and in alliance with Ana G. Méndez-Universidad Metropolitana, and the Universities Space Research Association. These data were processed on the ATLAS cluster of the Max-Planck-Institut für Gravitationsphysik/Albert-Einstein Institut, Hannover, Germany. L.G.S. and P.C.C.F. gratefully acknowledge financial support by the European Research Council for the ERC Starting grant BEACON under contract No. 279702. J.W.T.H. acknowledges funding for this work from ERC Starting grant DRAGNET (337062). Work at Cornell (J.M.C., S.C.) was supported by NSF grant 1104617. V.M.K. holds the Lorne Trottier Chair in Astrophysics and Cosmology and a Canadian Research Chair in Observational Astrophysics and received additional support from NSERC via a Discovery Grant and Accelerator Supplement, by FQRNT via the Centre de Recherche Astrophysique de Québec, and by the Canadian Institute for Advanced Research. Pulsar research at UBC is supported by NSERC Discovery and Discovery Accelerator Supplement Grants as well as by the CFI and CANARIE. P.L. acknowledges the support of IMPRS Bonn/Cologne and FQRNT B2.

REFERENCES

- Anderson, L. D., Bania, T. M., Balsler, D. S., et al. 2014, *ApJS*, 212, 1
- Bagchi, M., Nieves, A. C., & McLaughlin, M. 2012, *MNRAS*, 425, 2501
- Bannister, K. W., & Madsen, G. J. 2014, *MNRAS*, 440, 353
- Bhat, N. D. R., Cordes, J. M., Camilo, F., Nice, D. J., & Lorimer, D. R. 2004, *ApJ*, 605, 759
- Burke-Spolaor, S., & Bailes, M. 2010, *MNRAS*, 402, 855
- Burke-Spolaor, S., Bailes, M., Ekers, R., Macquart, J.-P., & Crawford, F., III 2011a, *ApJ*, 727, 18
- Burke-Spolaor, S., Bailes, M., Johnston, S., et al. 2011b, *MNRAS*, 416, 2465
- Cai, Y.-F., Sabancilar, E., Steer, D. A., & Vachaspati, T. 2012, *PhRvD*, 86, 043521
- Cordes, J. M., Freire, P. C. C., Lorimer, D. R., et al. 2006, *ApJ*, 637, 446
- Cordes, J. M., & Lazio, T. J. W. 2002, arXiv:astro-ph/0207156
- Cordes, J. M., & McLaughlin, M. A. 2003, *ApJ*, 596, 1142
- Deneva, J. S., Cordes, J. M., McLaughlin, M. A., et al. 2009, *ApJ*, 703, 2259
- Dowd, A., Sisk, W., & Hagen, J. 2004, in ASP Conf. Ser. 202, IAU Colloq. 177: Pulsar Astronomy—2000 and Beyond, ed. M. Kramer, N. Wex, & R. Wielebinski (San Francisco, CA: ASP), 275
- Falcke, H., & Rezzolla, L. 2014, *A&A*, 562, A137
- Finkbeiner, D. P. 2003, *ApJS*, 146, 407
- Haffner, L. M., Reynolds, R. J., & Tuftte, S. L. 1998, *ApJL*, 501, L83
- Haffner, L. M., Reynolds, R. J., Tuftte, S. L., et al. 2003, *ApJS*, 149, 405
- Hansen, B. M. S., & Lyutikov, M. 2001, *MNRAS*, 322, 695
- Hassall, T. E., Stappers, B. W., Hessels, J. W. T., et al. 2012, *A&A*, 543, A66
- Inoue, S. 2004, *MNRAS*, 348, 999
- Ioka, K. 2003, *ApJL*, 598, L79
- Kashiyama, K., Ioka, K., & Mészáros, P. 2013, *ApJL*, 776, L39
- Keane, E. F., Stappers, B. W., Kramer, M., & Lyne, A. G. 2012, *MNRAS*, 425, L71
- Kocz, J., Bailes, M., Barnes, D., Burke-Spolaor, S., & Levin, L. 2012, *MNRAS*, 420, 271
- Kulkarni, S. R., Ofek, E. O., Neill, J. D., Zheng, Z., & Juric, M. 2014, arXiv:1402.4766
- Lambert, H. C., & Rickett, B. J. 1999, *ApJ*, 517, 299
- Lazarus, P. 2013, in IAU Symp. 291, Neutron Stars and Pulsars: Challenges and Opportunities after 80 years, ed. J. van Leeuwen (Cambridge: Cambridge Univ. Press), 35

- Lazio, T. J. W., Ojha, R., Fey, A. L., et al. 2008, *ApJ*, 672, 115
- Loeb, A., Shvartzvald, Y., & Maoz, D. 2014, *MNRAS*, 439, L46
- Lorimer, D. R., Bailes, M., McLaughlin, M. A., Narkevic, D. J., & Crawford, F. 2007, *Sci*, 318, 777
- Lorimer, D. R., Karastergiou, A., McLaughlin, M. A., & Johnston, S. 2013, *MNRAS*, 436, L5
- Macquart, J.-P., & Koay, J. Y. 2013, *ApJ*, 776, 125
- Manchester, R. N., Hobbs, G. B., Teoh, A., & Hobbs, M. 2005, *AJ*, 129, 1993
- McLaughlin, M. A., Lyne, A. G., Lorimer, D. R., et al. 2006, *Natur*, 439, 817
- Paladini, R., Burigana, C., Davies, R. D., et al. 2003, *A&A*, 397, 213
- Popov, S. B., & Postnov, K. A. 2007, arXiv:0710.2006
- Rees, M. J. 1977, *Natur*, 266, 333
- Spitler, L. G., Cordes, J. M., Chatterjee, S., & Stone, J. 2012, *ApJ*, 748, 73
- Thornton, D., Stappers, B., Bailes, M., et al. 2013, *Sci*, 341, 53
- Weltevrede, P., Stappers, B. W., Rankin, J. M., & Wright, G. A. E. 2006, *ApJL*, 645, L149